Journal of Materials Chemistry A

Accepted Manuscript

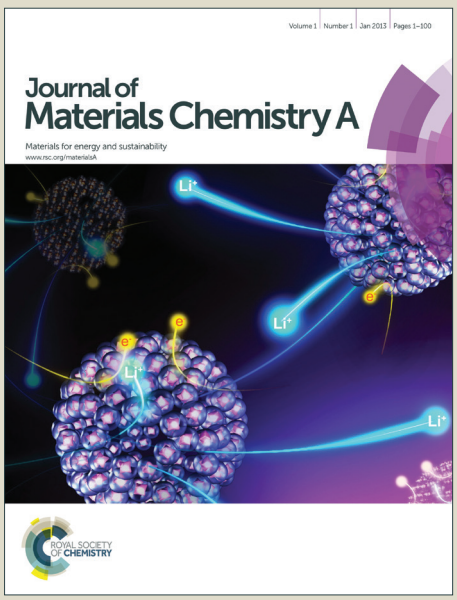

ROYAL SOCIETY OF CHEMISTRY

www.rsc.org/materialsA

Cite this: DOI: 10.1039/c0xx00000x

www.rsc.org/xxxxxx

ARTICLE TYPE

A highly selective and sensitive recyclable colorimetric Hg^{2+} sensor based on porphyrin-functionalized polyacrylonitrile fiber

Xiaoxing Liu,[a,b] Xiaojuan Liu,[a,b] Minli Tao*[a,b] and Wenqin Zhang*[a,b]

Received (in XXX, XXX) Xth XXXXXXXXX 20XX, Accepted Xth XXXXXXXXX 20XX

DOI: 10.1039/b000000x

A colorimetric Hg^{2+} sensor based on porphyrin-functionalized polyacrylonitrile fiber (CT_APP-PAN_AF) was prepared and investigated. This functional fiber sensor shows excellent selectivity and sensitivity towards Hg^{2+} over other common metal ions (Pb^{2+}, Ba^{2+}, Cd^{2+}, Ag^{+}, Zn^{2+}, Cu^{2+}, Ni^{2+}, Co^{2+}, Fe^{3+}, Mn^{2+}, Cr^{3+}, Ca^{2+}, Al^{3+} and Mg^{2+}). Upon addition of Hg^{2+}, a remarkable visual color change from red-brown to dark-green and significant detectable changes in the FTIR, UV and FL spectra of CT_APP-PAN_AF were observed. The naked-eye detection limit is as low as 20 ppb (1×10^{-7} mol L^{-1}), which is below the maximum contamination level of 50 ppb for mercury containing wastewater in China. This functional fiber sensor also exhibits excellent reusability and recyclability and can be repeatedly used for more than 50 times. The Hg^{2+} complexed sensor can be easily separated from the aqueous solution by simple filtration and reversed back by treating with dilute HCl. Furthermore, real water sample testing confirms the practical application of CT_APP-PAN_AF. In a word, the fiber sensor possesses the advantages of simplicity, rapidity, reusability as well as high selectivity and sensitivity.

Introduction

Mercury containing compounds widely used in industry are considered to be the most toxic materials to human health and environmental safety.[1] Among them, the water soluble Hg^{2+} is one of the most common and stable forms of mercury pollution.[2] Exposure to Hg^{2+} even at very low concentrations still has potential risks for human beings.[3] Traditional Hg^{2+} detection methods including atomic absorption spectroscopy (AAS), atomic fluorescence spectrometry (AFS) and inductively coupled plasma mass spectrometry (ICPMS) had been widely used.[4-6] However, these methods require expensive equipments and complicated sample treatment, which limit their applications for rapid and in-situ analysis.[7] Recently, a number of new methods for the detection of Hg^{2+} have been developed, such as fluorescence methods, electrochemical assays and colorimetric strategies.[8-15] Among them, growing attention has been paid to the colorimetric strategies due to the direct determination of Hg^{2+} by a color change without the necessity of special equipment. For in situ applications, solid-state sensor materials can provide portability and operational simplicity. Many sensors for heavy metal ions,[16-19] especially for Hg^{2+},[20-24] have been either physically adsorbed or chemically immobilized onto solid supports recently. However, most of them have significant drawbacks, such as breakage of probes during real-time applications, high price, low selectivity and poor reusability. Therefore, developing new colorimetric mercury-specific sensors based on solid materials with high selectivity and sensitivity is of great importance and highly desirable.

Commercially available polyacrylonitrile fiber (PANF) with its main advantage compared to the granular resins is a unique combination of large surface areas, extremely fast rate of sorption, low cost and easily to be separated.[25] Furthermore, it contains an abundance of cyano groups, which can be easily transformed into various functional moieties (carboxyl, amide, amidoxime, etc.).[26] These properties make PANF an excellent candidate as supporting material for heavy metal ion detection and absorption.[27-30]

Porphyrin derivatives have been extensively used as fluorophores in the detection of heavy metal ions (Cd^{2+}, Pb^{2+} and Hg^{2+}).[31-37] Because the porphyrins possess advantageous photophysical characteristics such as tunable fluorescence emission with a concomitant modification of molecular structure, large Stokes shift that minimize the effects of the background fluorescence and quite different emission properties of the metallo- and free base porphyrin.[1, 38-40] Unfortunately, most of the fluorophores based on single emission intensity changes tend to be affected by a variety of factors such as instrumental efficiency, probe molecule concentration, its stability under illumination and microenvironment around probe molecule.[34] Furthermore, fluorophores have been reported in "homogeneous system" as solution state, which is unrecycled.[41] In recent years, some efforts have been made to develop the porphyrins based solid-state colorimetric sensors for heavy metal ions. A 5-(4-aminophehyl)-10,15,20-triphenyporphyrin immobilized on Fe_3O_4@SiO_2 core magnetic microspheres has been proved to behave high selectivity towards Hg^{2+} over other metal ions.[42] However, due to the requirement of organic solvent to dissolve the water-insoluble

microspheres, it is inconvenience to monitor continuously dispersed water resources. Moreover, almost no color change was observed when the concentration of Hg^{2+} is lower than 4×10^{-5} mol L^{-1}, therefore it is not suitable for the detection of trace amounts of Hg^{2+}.

Herein, we report the synthesis and application of a novel designed Hg^{2+} responsive colorimetric fiber (CT_APP-PAN_AF) based on porphyrins functionalized PANF (Scheme 1). Dipping the sensor in Hg^{2+} solution results in a remarkable color-change with high selectivity and sensitivity in the presence of various environmentally relevant metal ions.

Scheme 1 Preparation of CT_APP-PAN_AF.

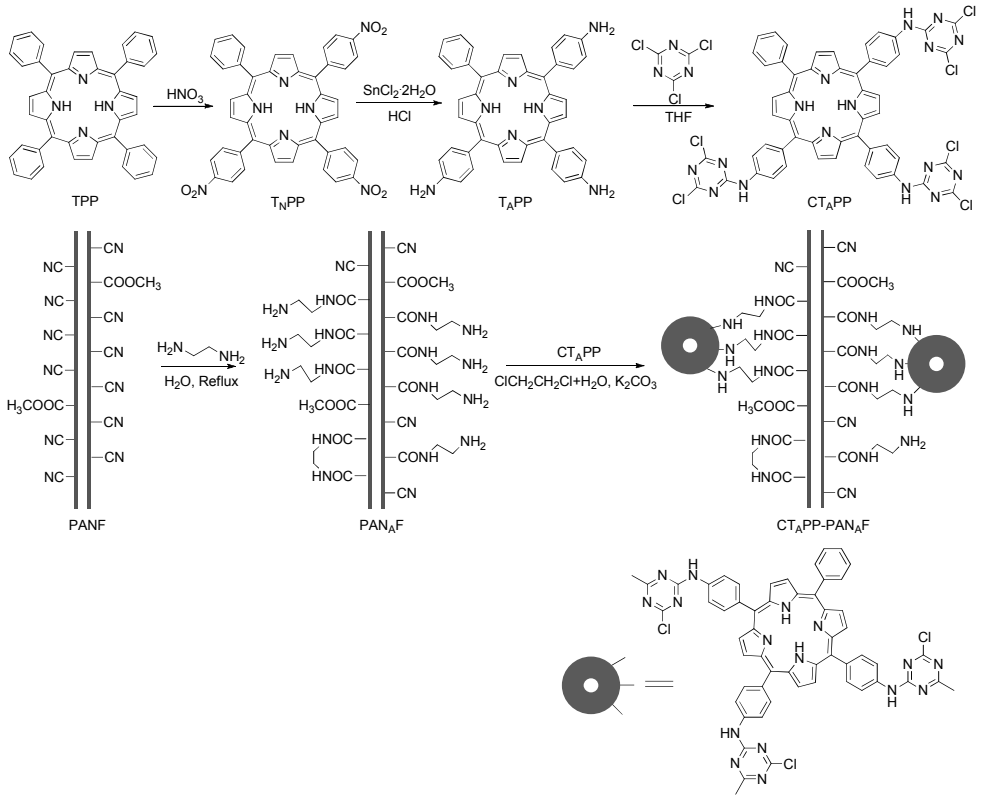

Experimental

Reagents

PANF with a length of 10 cm and a diameter of 20±0.5 μm was obtained from the Fushun Petrochemical Corporation of China. All reagents used were analytical grade and employed without further purification. All water used was distilled water except those specialized.

Apparatus and instruments

The Fourier transform infrared (FTIR) spectra were obtained with an AVATAR 360 FTIR spectrometer (Thermo Nicolet). The Elemental analysis (EA) were performed on a vario micro cube (Elementar). A scanning electron microscope (SEM) (Hitachi, model S-4800) was used to characterize the surface of the fiber. The X-ray powder diffraction spectra (XRD) were recorded with a D/MAX-2500 X-ray diffractometer. The UV-vis spectra were obtained with a TU-1901 UV-vis spectrometer, equipped with an integrating sphere. The Fluorescence emission spectra (FL) were recorded on a Hitachi F-4500 Fluotrscence Spectrophotometer. ^{1}H NMR spectra were recorded on an AVANCE III instrument (Bruker, 400 MHz) using TMS as the internal standard. Mass spectra were recorded on an Autoflex tof/tof III matrix assisted laser desorption ionization time-of-flight (MALDI-TOF) mass spectrometer, in *m/z*. The pH values were determined with a Model PHS-3C pH meter. All photos were recorded by a Canon PowerShot SX700 HS digital camera.

Synthesis of the Porphyrin-functionalized polyacrylonitrile fiber

The synthesis of the colorimetric fiber was carried out in two steps as follows.

Step 1: the amination of PANF

Dried PANF (1.0 g), ethylenediamine (10 mL) and water (20 mL) were placed in a three-necked flask. After the mixture was refluxed for 3.5 h, the fiber was filtered and washed with water (60-70 ^{o}C) until neutral, and then dried at 60 ^{o}C under vacuum over night to get the aminated fiber (PAN_AF). The weight gain of PAN_AF based on PANF was 9.8%.

Step 2: the immobilization of the 5,10,15-Tris[4-(3,5-dichlorotriazinyl)aminophenyl]-20-phenylporphyrin (CT_APP)

Dried PAN_AF (0.3 g), CT_APP (1.0 g, see ESI† 1 and 2), K_2CO_3 (0.5 g), 1,2-dichloroethane (15 mL) and water (10 mL) were placed in a three-necked flask. The mixture was stirred and refluxed for 12 h. After the mixture was cooled, the fiber was filtered and washed with CH_2Cl_2 (10 mL) three times. Then the fiber was washed in a Soxhlet apparatus for 48 h with

CH_2Cl_2/methanol (1:1 v/v) in order to remove the residual unreacted CT_APP molecules and then dried at 60 °C under vacuum over night to get the porphyrin-functionalized polyacrylonitrile fiber (CT_APP-PAN_AF) with a weight gain of 16.7% based on PAN_AF.

Preparation of solutions

Perchlorate or nitrate salts of Pb^{2+}, Hg^{2+}, Ba^{2+}, Cd^{2+}, Ag^{+}, Zn^{2+}, Cu^{2+}, Ni^{2+}, Co^{2+}, Fe^{3+}, Mn^{2+}, Cr^{3+}, Ca^{2+}, Al^{3+} and Mg^{2+} were used. Stock solution of Hg^{2+} (1×10^{-2} mol L^{-1}) was prepared by dissolving an appropriate amount of $Hg(ClO_4)_2\bullet3H_2O$ in water and adjusting the volume to 100 mL in a volumetric flask. This was further diluted to 1×10^{-3} to 1×10^{-7} mol L^{-1} stepwisely. The pH was adjusted by 0.1 mol L^{-1} HNO_3 and 0.1 mol L^{-1} NaOH. The complex solutions of $[EDTA\text{-}Hg]^{2-}$, $[HgI_4]^{2-}$ and $[Hg(S_2O_3)_4]^{6-}$ were prepared by dissolving 10^{-3} mol $Hg(ClO_4)_2\bullet3H_2O$ with 10^{-2} mol EDTA, KI and $Na_2S_2O_3\bullet5H_2O$ in water and adjusting the volume to 1 L. This was further diluted to 1×10^{-5} mol L^{-1}.

Reversibility of Hg^{2+} complexed CT_APP-PAN_AF

To verify its reusability, the CT_APP-PAN_AF was immersed into a solution of 1×10^{-3} mol L^{-1} Hg^{2+} (20 mL) along with a color change from red-brown to dark-green, after which the Hg^{2+} complexed CT_APP-PAN_AF (CT_APP-PAN_AF-Hg) was desorbed by dipping it in 1.0 mol L^{-1} HCl (20 mL) for 1 h. Then the fiber was washed with 10 mL of water, 10 mL of 1.0 mol L^{-1} Na_2CO_3 and water until neutral.

Results and discussion

Synthesis of the colorimetric fiber

CT_APP was covalently bonded to PANF via a simple two-step strategy. The extent of modification is measured by the weight gain and the acid exchange capacity of the produced fiber. Weight gain = $[(W_2\text{-}W_1)/W_1]\times100\%$. For the amination step, W_1 and W_2 are the weights of PANF and PAN_AF, respectively. For the immobilization step, W_1 and W_2 are the weights of PAN_AF and CT_APP-PAN_AF, respectively.

As discussed in our previous work, the amination is strongly influenced by the reaction time and temperature.[43] Taking the large steric hindrance of CT_APP into account, PAN_AF with a weight gain of 9.8% was obtained successfully by surface layer modification of PANF, and the corresponding acid exchange capacity in 0.1 mol L^{-1} HCl was determined to be 1.1 mmol g^{-1} (see ESI† 3).

In the immobilization step, the CT_APP is covalently bonded inside the surface layer of PAN_AF. Owing to the replacement of the second chloro atom of cyanuric chloride requires higher reaction temperature, 1,2-dichloroethane is selected as solvent instead of CH_2Cl_2. A certain amount of water is added to swell the fiber effectively. In order to make an excellent combine of selectivity and on-site real-time detection for Hg^{2+}, CT_APP-PAN_AF with a weight gain of 16.7% was selected for further studies, and the corresponding functionality is 0.14 mmol g^{-1} (see ESI† 4).

Characterization of the fiber

Elemental analysis (EA). The EA data of PANF, PAN_AF, CT_APP-PAN_AF, CT_APP-PAN_AF-Hg (Hg^{2+} complexed CT_APP-PAN_AF), CT_APP-PAN_AF-1 (after one iteration of absorption and desorption) and CT_APP-PAN_AF-50 (after 50 iterations of absorption and desorption) are shown in Table 1. Compared to the original PANF, the carbon and nitrogen contents of PAN_AF decrease and the hydrogen content increases as expected (Table 1, entries 1 and 2). After the immobilization of the CT_APP in PAN_AF, the sum of carbon, hydrogen and nitrogen contents decrease significantly (Table 1, entry 3), owing to the introduction of chloro atoms. In CT_APP-PAN_AF-Hg (Table 1, entry 4), a further decrease in the sum of the three element contents can be act as an evidence to prove the absorption of mercury in CT_APP-PAN_AF. What is more, the EA data of CT_APP-PAN_AF-1 (Table 1, entry 5) and CT_APP-PAN_AF-50 (Table 1, entry 6) stay almost the same with that of CT_APP-PAN_AF, which indicates that there is no significant outflowing of the CT_APP from PAN_AF after being recycled 50 iterations.

Table 1 EA data of PANF, PAN_AF, CT_APP-PAN_AF, CT_APP-PAN_AF-Hg, CT_APP-PAN_AF-1 and CT_APP-PAN_AF-50.

Entry	Sample	C(%)	H(%)	N(%)	Sum(%)
1	PANF	70.75	5.94	26.12	102.81
2	PAN_AF	65.79	6.32	22.46	94.57
3	CT_APP-PAN_AF	55.76	6.35	17.43	79.54
4	CT_APP-PAN_AF-Hg	36.65	3.88	11.17	51.70
5	CT_APP-PAN_AF-1	56.17	6.26	17.39	79.82
6	CT_APP-PAN_AF-50	54.37	5.98	17.02	77.37

Fourier transform infrared spectroscopy (FTIR). The PANF, PAN_AF, CT_APP-PAN_AF, CT_APP-PAN_AF-Hg, CT_APP-PAN_AF-1 and CT_APP-PAN_AF-50 samples were pulverized by cutting and then prepared into KBr pellets. Their FTIR spectra were shown in Fig. 1. Comparing the FTIR spectrum of PAN_AF (Fig. 1b) with that of PANF (Fig. 1a), the most striking change is the broad absorption peak around 3290 cm^{-1}, which is characterized as the N-H stretching vibration. For CT_APP-PAN_AF (Fig. 1c), the intensity of the peaks at 1560 cm^{-1} and 1650 cm^{-1} are increased obviously compared with that of PAN_AF, which is contributed by the stretching vibration absorption of aromatic ring skeleton and confirms further the successful immobilization of the CT_APP in PAN_AF. The CT_APP-PAN_AF-Hg (Fig. 1d) exhibits a new strong absorption peak at 1090 cm^{-1} that is assigned to the characteristic absorption peak of metal porphyrin complexes.[44, 45] The FTIR spectra of CT_APP-PAN_AF-1 (Fig. 1e) and CT_APP-PAN_AF-50 (Fig. 1f) are quite similar to the spectrum of CT_APP-PAN_AF, which indicates that the colorimetric sensor can be reused more than 50 times without significant change.

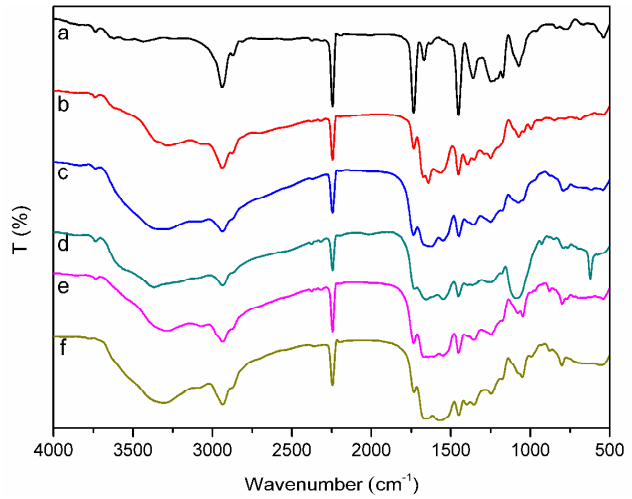

Fig. 1 FTIR spectra of (a) PANF, (b) PAN_AF, (c) CT_APP-PAN_AF, (d) CT_APP-PAN_AF-Hg, (e) CT_APP-PAN_AF-1 and (f) CT_APP-PAN_AF-50.

Scanning electron microscopy (SEM). Fig. 2 presents the SEM images of PANF, PAN_AF, CT_APP-PAN_AF, CT_APP-PAN_AF-Hg, CT_APP-PAN_AF-1 and CT_APP-PAN_AF-50. After the amination and CT_APP immobilization, the surface of the fiber becomes rougher and the diameter of PAN_AF (Fig. 2b) and CT_APP-PAN_AF (Fig. 2c) extends obviously compared to the original PANF (Fig. 2a). Furthermore, with the repeated use of CT_APP-PAN_AF, the damage to the surface of the fiber increases (Fig. 2e and 2f). However, the overall integrity of the fiber is untouched and retains enough physical durability to meet the needs for further application.

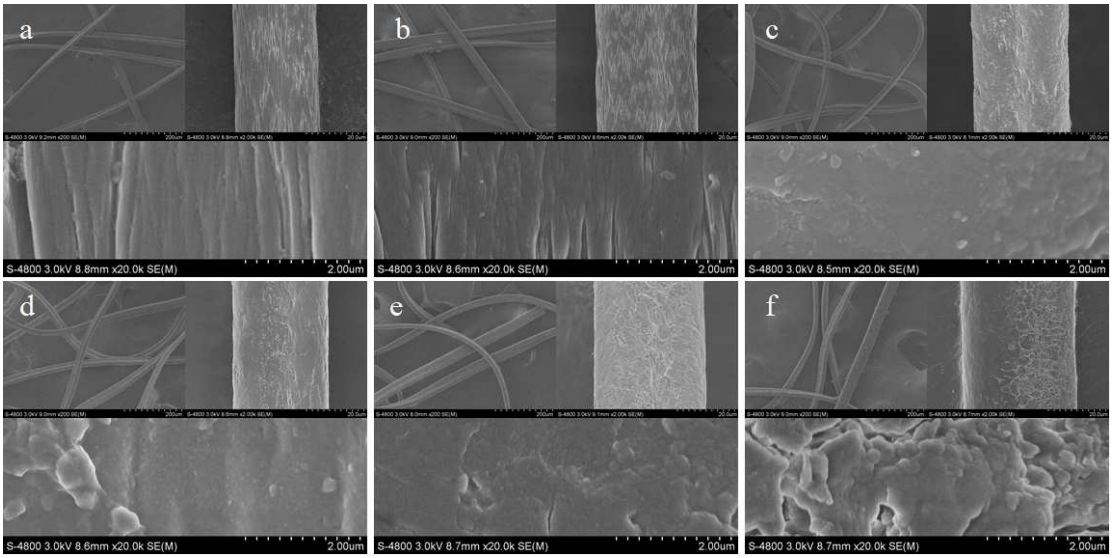

Fig. 2 SEM images of (a) PANF, (b) PAN_AF, (c) CT_APP-PAN_AF, (d) CT_APP-PAN_AF-Hg, (e) CT_APP-PAN_AF-1 and (f) CT_APP-PAN_AF-50.

X-ray diffraction (XRD). The XRD spectrum of PANF (Fig. 3a) shows an intense reflection peak at 2θ=17° which corresponds to the (100) diffraction of the hexagonal lattice formed by parallel close packing of molecule rods, indicating that PANF adopts a stiff rod-like conformation due to the intermolecular repulsion of the nitrile dipoles.[46] After the amination, the intensity of the crystalline peak decreases (Fig. 3b), which indicates a decrease in the polar interaction between molecule chains during the reaction and the breakage of the outer crystal region.[47] CT_APP-PAN_AF (Fig. 3c) has almost the same reflection peak (2θ=17°) as PAN_AF, implying that the inner crystal region of this fiber is not damaged further after the immobilization of CT_APP. The reflection peak disappeares completely after the complexation with Hg^{2+} (Fig. 3d), but can be fully restored after treating with dilute HCl (Fig. 3e). Furthermore, only a small decrease is observed after being used 50 times (Fig. 3f), which further verifies the above deduction and indicates that the intensity of this color-changing fiber has been maintained.

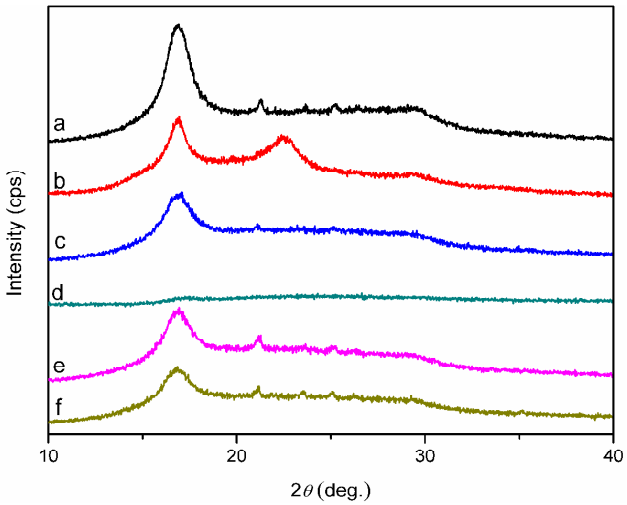

Fig. 3 XRD spectra of (a) PANF, (b) PAN_AF, (c) CT_APP-PAN_AF, (d) CT_APP-PAN_AF-Hg, (e) CT_APP-PAN_AF-1 and (f) CT_APP-PAN_AF-50.

Colorimetric detection of Hg^{2+}

Selectivity. The metal ion selectivity of the porphyrin-functionalized fiber was evaluated by testing the response of the assay to common environmentally relevant ions, including Pb^{2+}, Hg^{2+}, Ba^{2+}, Cd^{2+}, Ag^{+}, Zn^{2+}, Cu^{2+}, Ni^{2+}, Co^{2+}, Fe^{3+}, Mn^{2+}, Cr^{3+}, Ca^{2+}, Al^{3+} and Mg^{2+} ions. As shown obviously in Fig. 4, when immersed in the Hg^{2+} solution with a concentration of 1×10^{-3} mol L^{-1}, the fiber changed its color immediately from red-brown to dark-green. To our delighted surprise, when the concentration of the other ions were increased to 10 times larger than that of Hg^{2+}, still no color change was observed. These observations clearly turn out that the functionalized fiber has excellent visual selectivity for Hg^{2+}, which allows simple on-site real-time detection of Hg^{2+} by the naked-eyes.

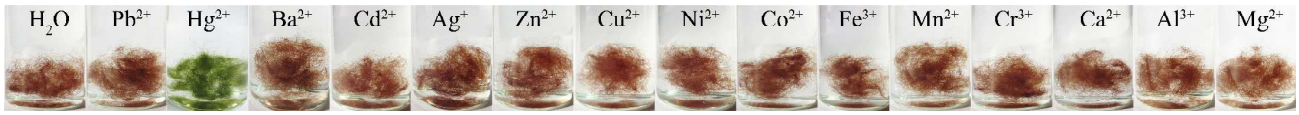

Fig. 4 Color change of $CT_APP\text{-}PAN_AF$ in the presence of different ions at pH=5.0. The concentration of Hg^{2+} is 1×10^{-3} mol L^{-1}. The concentration of other metal ions is 1×10^{-2} mol L^{-1}.

Then the fiber sensor was examined by competition experiments by adding Hg^{2+} to a mixture of 14 kinds of commonly existing metal ions including Pb^{2+}, Hg^{2+}, Ba^{2+}, Cd^{2+}, Ag^{+}, Zn^{2+}, Cu^{2+}, Ni^{2+}, Co^{2+}, Fe^{3+}, Mn^{2+}, Cr^{3+}, Ca^{2+}, Al^{3+} and Mg^{2+} (each at a concentration of 1×10^{-2} mol L^{-1}). In the presence of miscellaneous competitive metal ions, the sensor still resulted in a similar visual color change (Fig. 5A d), while in the miscellaneous competitive ions without Hg^{2+}, the color of the fiber sensor doesn't change any more (Fig. 5A c). The competition experiments demonstrate that the fiber sensor has predominant selectivity to Hg^{2+} and strong capability against the existence of the other interference metal ions.

The super selectivity of the sensor was further investigated by the FTIR, UV and FL spectra. After being treated with Hg^{2+} solution or metal ion mixture containing Hg^{2+}, the FTIR spectra exhibit a new strong absorption peak at 1090 cm^{-1} (Fig. 5B b and d) that is assigned to the characteristic absorption peak of porphyrin-Hg complex. The UV spectrum of $CT_APP\text{-}PAN_AF$ (Fig. 5C a) exhibits a typical absorption spectrum of metal-free porphyrin with a strong Soret band at 426 nm and four weak Q bands at 525, 562, 599 and 656 nm, respectively. With the decrease and the disappearance of Q bands, the absorption bands ascribed to porphyrin-Hg complex (at 460 nm) appear after being treated with Hg^{2+} (Fig. 5C b and d). More notably, the FL bands at 630 and 730 nm are quenched completely (Fig. 5D b and d).

In contrast to the significant color and spectral changes as observed for those cases containing Hg^{2+} (Fig. 5b and 5d), very little change was observed upon exposure to the mixture of competitive ions without Hg^{2+} (Fig. 5c). These results suggest that the immobilized porphyrin only complex with Hg^{2+} and subsequently change the color and spectra of the fiber sensor, the competitive ions had no interference to the detection of Hg^{2+}, which demonstrated that $CT_APP\text{-}PAN_AF$ is an outstanding visual sensor for selective recognization of Hg^{2+}.

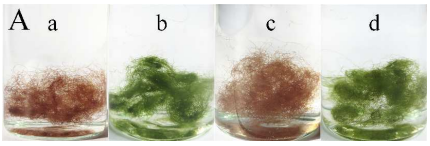

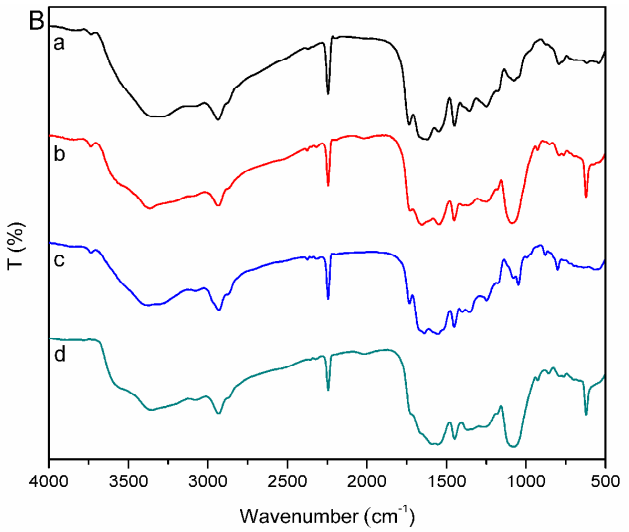

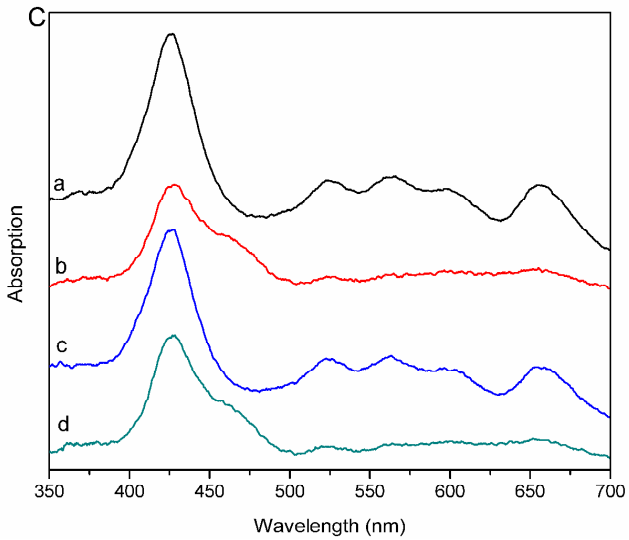

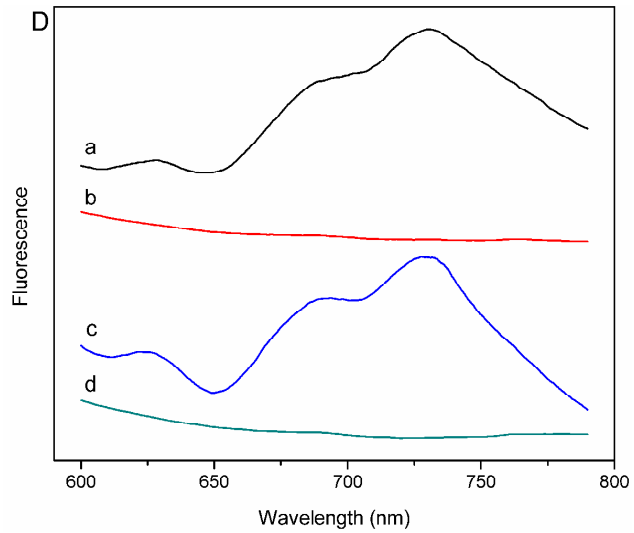

Fig. 5 (A) Color change, (B) FTIR, (C) UV, (D) FL (λ_{ex}=420 nm) spectra of $CT_APP\text{-}PAN_AF$ after being immersed (a) in water, (b) in Hg^{2+} solution at 1×10^{-2} mol L^{-1}, (c) in a mixture solution of 14 kinds of competitive ions without Hg^{2+} at 1×10^{-2} mol L^{-1} for each, (d) in a mixture solution of 14 kinds of competitive ions with Hg^{2+} at 1×10^{-2} mol L^{-1} for each.

Reusability. The reusability of the sensor is also one of the essential aspects for sensor applications. To evaluate further the reversibility of the fiber, dilute HCl was used as the desorption agent for removal of Hg^{2+} from Hg^{2+} complexed $CT_APP\text{-}PAN_AF$. As shown in Fig. 6c, the color and spectra of $CT_APP\text{-}PAN_AF$ in the presence of Hg^{2+} were found to be almost reversible. In addition, after 50 iterations of absorption-desorption, the fiber still responds very well to Hg^{2+} in water. The color and spectra of $CT_APP\text{-}PAN_AF\text{-}50$ (Fig. 6d) have no significant difference compared with those of $CT_APP\text{-}PAN_AF$ (Fig. 6a) and $CT_APP\text{-}PAN_AF\text{-}1$ (Fig. 6c). These results are in good agreement with the EA data (Table 1, entry 3-6) and XRD spectra (Fig. 3c-3f) results, thus, indicate that the fiber can be reused more than 50 times.

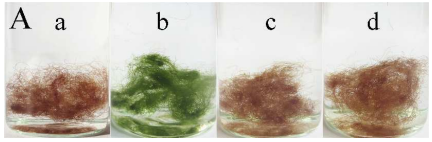

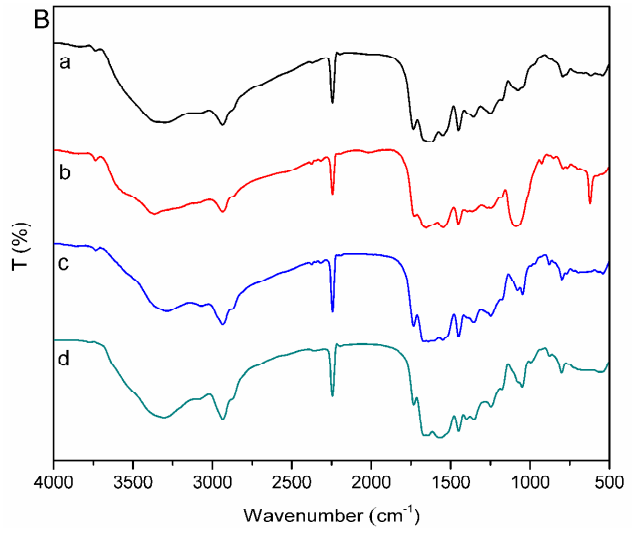

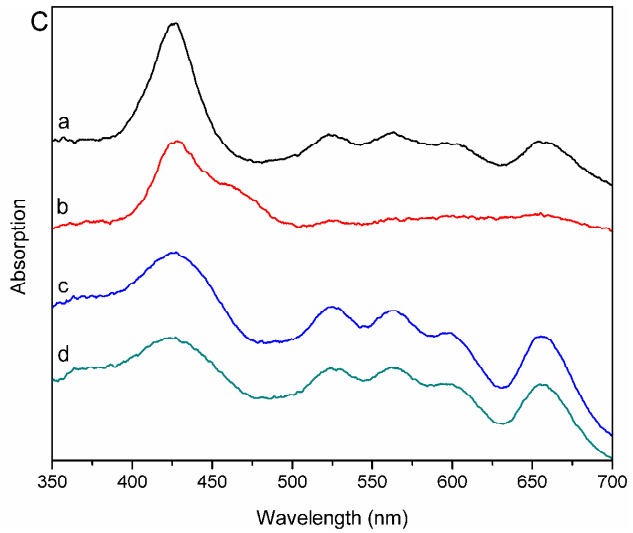

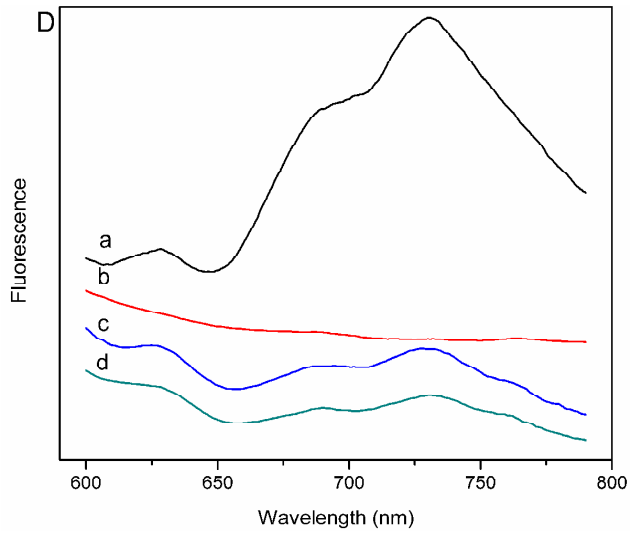

Fig. 6 (A) Color change, (B) FTIR, (C) UV, (D) FL (λ_{ex}=420 nm) spectra of $CT_APP\text{-}PAN_AF$ after being immersed (a) in water, (b) in Hg^{2+} solution at 1×10^{-2} mol L^{-1}, (c) in water after one iteration of absorption and desorption, (d) in water after 50 iteration s of absorption and desorption.

Response time. In general, the interaction of the porphyrins with metal ion in aqueous solution at room temperature is slow. However, when $CT_APP\text{-}PAN_AF$ was soaked in a solution of 1×10^{-3} mol L^{-1} Hg^{2+}, distinctive color change from red-brown to dark-green was observed within 5 s (Fig. 7) and the color changes deeply along with the elongation of contact time. The fast response of $CT_APP\text{-}PAN_AF$ toward Hg^{2+} might be ascribed to the good kinetic property which is caused by the short diffusion path of the analyte into the fiber sensor. Therefore, this sensor can be used for real-time detection of Hg^{2+} in water.

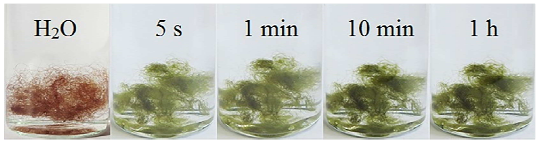

Fig. 7 Response time of $CT_APP\text{-}PAN_AF$ with Hg^{2+} (1×10^{-3} mol L^{-1}, pH =5.0).

Sensitivity. The color change of $CT_APP\text{-}PAN_AF$ after addition of Hg^{2+} is attributed by the formation of Hg-porphyrin complex

with a stoichiometry of one Hg^{2+} per porphyrin moiety.[48] Along with the gradient decrease of the concentration of Hg^{2+} from 1×10^{-4} to 1×10^{-7} mol L^{-1}, the volume of solutions required is increased accordingly to ensure that there are sufficient amount of Hg^{2+} to be complexed by CT_APP-PAN_AF, correspondingly the response time increases to 15 min, 1 h, 5 h and 24 h, respectively (see ESI† 5). Fig. 8 presents the colorimetric response of the fiber toward low concentrations of Hg^{2+} in tap water where the amount of Hg^{2+} is sufficient. In this case, the colorimetric detection limit for Hg^{2+} is as low as 1×10^{-7} mol L^{-1} (20 ppb) based on the naked-eye observation.

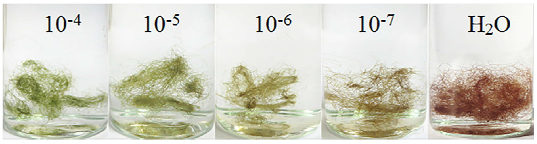

Fig. 8 Color change of CT_APP-PAN_AF with Hg^{2+} at low concentrations (mole number of Hg^{2+} is fixed, pH=6.8).

When the mole number of Hg^{2+} in solutions decreases gradually with fixed volume, i.e. 1 L, the response time is 15 min, 1 h and 15 h, respectively (see ESI† 5). Fig. 9 presents the colorimetric response of the fiber in this case, accordingly, the visual detection limit increases to 1×10^{-6} mol L^{-1}.

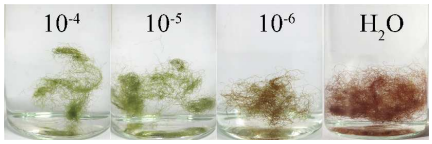

Fig. 9 Color change of CT_APP-PAN_AF with Hg^{2+} at low concentrations (volume of solutions is fixed, pH=6.8).

In both cases, the response time increases gradually with the decreasing of Hg^{2+} concentration, so the concentration of Hg^{2+} can be estimated according to the response time. Moreover, CT_APP-PAN_AF is more convenient to monitor continuously dispersed water resources, as long as sufficient amount of Hg^{2+} is provided, color change of the fiber is observed.

pH effect. The pH values of the environment around the sensor usually show somewhat of an effect on its performance toward target ions due to the protonation or deprotonation reaction and the hydrolysis of metal ions under basic condition.[49] The effect of pH values was therefore investigated. Solutions that contain a specific concentration (1×10^{-5} mol L^{-1}) of Hg^{2+} were adjusted to a pH range from 3.0 to 11.0. As shown in Fig. 10, acidity and alkalinity do not affect the determination of Hg^{2+}. These results indicate that this sensor can be used in a wide range of pH values, which is very convenient for practical applications in actual samples because there is no need for special adjustment of the pH.

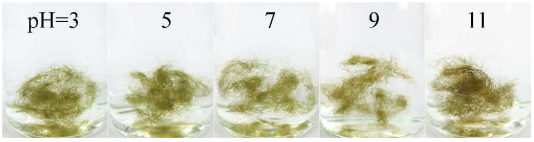

Fig. 10 Color change of CT_APP-PAN_AF with Hg^{2+} (1×10^{-5} mol L^{-1}) at different pH.

Practical application. Most of the developed analytical assays may fail in real samples because of the negative incidence of the ionic strength and the presence of exchangeable ligands.[50] To confirm the practical application of CT_APP-PAN_AF, a test on the real water sample was performed. The water sample taken from Weijin River (Tianjin, China) was used without any treatment, no obvious signal for Hg^{2+} was observed. After being spiked with concentrated standard Hg^{2+} solution, the concentration of Hg^{2+} in the real water sample was 1×10^{-5} mol L^{-1}. As shown in Fig. 11, a similar color change was observed as standard water sample, which reveals that the fiber is applicable for practical Hg^{2+} detection with other potentially competing species coexisting.

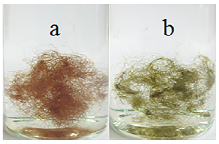

Fig. 11 Color change of CT_APP-PAN_AF (a) in real water sample, (b) spiked with Hg^{2+} (1×10^{-5} mol L^{-1}) in real water sample.

Complexation ability. The strong complexion ability was investigated by determination the color change of CT_APP-PAN_AF in the presence of $[EDTA\text{-}Hg]^{2-}$, $[HgI_4]^{2-}$ and $[Hg(S_2O_3)_4]^{6-}$ at 1×10^{-5} mol L^{-1}. Though the high stability of the complexes (stability constants are 21.8, 29.83 and 33.24, respectively), color change was observed as before (Fig. 12), which indicates that this colorimetric fiber has strong complexion ability for Hg^{2+}.

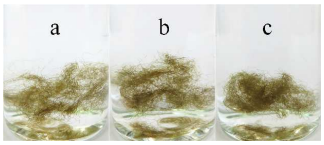

Fig. 12 Color change of CT_APP-PAN_AF in the presence of (a) $[EDTA\text{-}Hg]^{2-}$, (b) $[HgI_4]^{2-}$ and (c) $[Hg(S_2O_3)_4]^{6-}$ (1×10^{-5} mol L^{-1}, pH=6.8).

The color-changing mechanism of CT_APP-PAN_AF. From the perspective of coordination chemistry, the porphyrin ligand has turned out to be very versatile, and almost all metals have been combined with porphyrins.[51] But porphyrin derivatives are widely used as fluorescent and colorimetric metal-responsive sensors for the selective detection of metal ions.[31-37] This is owing to the introduction of different substituents at porphyrin's periphery can tune its optical and electrochemical properties and thus enhance its selective response to definite metal ions. In this paper, the CT_APP immobilized PAN_AF shows a significant color change in the presence of Hg^{2+}, whereas, due to the poor solubility in water, free CT_APP remains in dark purple without any perceptible color change even at higher concentration of Hg^{2+} (1×10^{-2} mol L^{-1}). Although a dark-green color change was observed by adding CH_2Cl_2 to dissolve the water-insoluble free CT_APP, the response time is increased at least ten times longer than that of CT_APP-PAN_AF, of course, the free CT_APP is difficult to be recycled. These results incontestably demonstrate that the immobilization significantly improves the responsibility, compatibility and reusability of porphyrin to Hg^{2+}.

CT_APP-PAN_AF shows excellent selectivity towards Hg^{2+} in both color and spectral changes is probably due to the suitable coordination geometry conformation of the sensor, which provides a more "soft" environment to host the softest Hg^{2+} more easily. According to the literature, the reversible color change of CT_APP-PAN_AF after addition of Hg^{2+} can be attributed to the

complex formation between Hg^{2+} and porphyrin moiety, which is a result of metal binding to four N-atoms in the porphyrin ring (Scheme 2).[48] Moreover, the microenvironment constructed by the porphyrin moieties and the unreacted aminoethyl groups helps a lot to improve the compatibility, reusability, sensitivity and selectivity of the fiber sensor.

Scheme 2 The color-changing mechanism of CT_APP-PAN_AF.

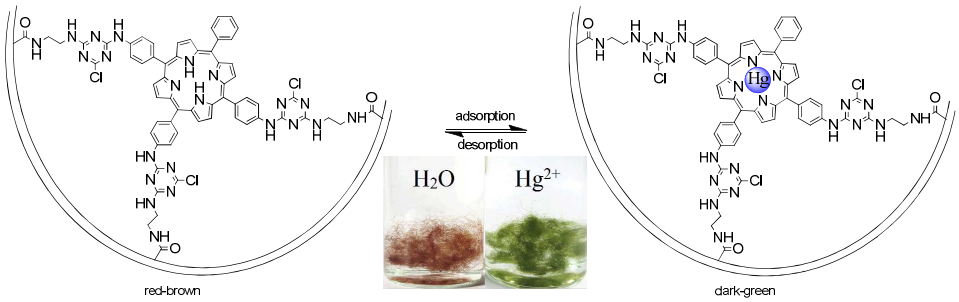

Conclusions

A porphyrin-functionalized polyacrylonitrile fiber (CT_APP-PAN_AF) was synthesized. Investigations reveal that CT_APP-PAN_AF can act as a superior colorimetric sensor which provides rapid, selective and sensitive detection of Hg^{2+} in the presence of other competitive metal ions with a remarkable visual colour change from red-brown to dark-green. The formation of the porphyrin-Hg complex was further confirmed by the FTIR, UV and FL spectra. Furthermore, CT_APP-PAN_AF works well over a wide pH range from 3.0 to 11.0 and can be reused for more than 50 times. The naked-eye detection limit of CT_APP-PAN_AF for Hg^{2+} is 1×10^{-7} mol L^{-1} (20 ppb), therefore it can be applied in the determination of trace amounts of Hg^{2+} in water samples. The successful detection of 1×10^{-5} mol L^{-1} Hg^{2+} dissolved in a real river water sample confirms that this fiber sensor has practical usability. Given these attractive characteristics, this facile, low cost and solid-state Hg^{2+} detecting sensor represents a great advance for the in-situ monitoring of Hg^{2+} in environmental applications.

Acknowledgements

The authors are grateful for the financial support from the National Natural Science Foundation of China (No: 21306133); Tianjin Research Program of Application Foundation and Advanced Technology (No: 14JCYBJC22600).

Notes and references

a Department of Chemistry, School of Sciences, Tianjin University, Tianjin, 300072, P. R. China. Fax: +86-22-27403475; Tel: +86-22-27890922; E-mail: mltao@tju.edu.cn; zhangwenqin@tju.edu.cn
b Collaborative Innovation Center of Chemical Science and Engineering (Tianjin), Tianjin 300072, P. R. China.

† Electronic Supplementary Information (ESI) available: [Synthesis of 5,10,15-Tris(4-aminophenyl)-20-phenylporphyrin (T_APP); Synthesis of 5,10,15-Tris[4-(3,5-dichlorotriazinyl)aminophenyl]-20-phenylporphyrin (CT_APP); Acid exchange capacity of the produced fiber; Functionality of CT_APP-PAN_AF; Sensitivity study]. See DOI: 10.1039/b000000x/

1 H. N. Kim, W. X. Ren, J. S. Kim and J. Yoon, *Chem. Soc. Rev.*, 2012, **41**, 3210-3244.
2 X. Guo, X. Qian and L. Jiat, *J. Am. Chem. Soc.*, 2004, **126**, 2272-2273.
3 H. H. Harris, I. J. Pickering and G. N. George, *Science*, 2003, **301**, 1203-1203.
4 K. Leopold, M. Foulkes and P. J. Worsfold, *Anal. Chem.*, 2009, **81**, 3421-3428.
5 Z. Li, Q. Wei, R. Yuan, X. Zhou, H. Liu, H. Shan and Q. Song, *Talanta*, 2007, **71**, 68-72.
6 Y. Zhao, J. Zheng, L. Fang, Q. Lin, Y. Wu, Z. Xue and F. Fu, *Talanta*, 2012, **89**, 280-285.
7 Y. Zhou, H. Dong, L. Liu, M. Li, K. Xiao and M. Xu, *Sens Actuators, B*, 2014, **196**, 106-111.
8 G. Mor-Piperberg, R. Tel-Vered, J. Elbaz and I. Willner, *J. Am. Chem. Soc.*, 2010, **132**, 6878-6879.
9 J. Gong, T. Zhou, D. Song, L. Zhang and X. Hu, *Anal. Chem.*, 2010, **82**, 567-573.
10 M. Zhang, M. Yu, F. Li, M. Zhu, M. Li, Y. Gao, L. Li, Z. Liu, J. Zhang, D. Zhang, T. Yi and C. Huang, *J. Am. Chem. Soc.*, 2007, **129**, 10322-10323.
11 Y. Si, X. Wang, Y. Li, K. Chen, J. Wang, J. Yu, H. Wang and B. Ding, *J. Mater. Chem. A*, 2014, **2**, 645-652.
12 T. Ye, C. He, Y. Qu, Z. Deng, Y. Jiang, M. Li and X. Chen, *Analyst*, 2012, **137**, 4131-4134.
13 H. Xu, Y. Wang, X. Huang, Y. Li, H. Zhang and X. Zhong, *Analyst*, 2012, **137**, 924-931.
14 F. Zhang, L. Zeng, C. Yang, J. Xin, H. Wang and A. Wu, *Analyst*, 2011, **136**, 2825-2830.
15 L. Q. Xu, K. G. Neoh, E. T. Kang and G. D. Fu, *J. Mater. Chem. A*, 2013, **1**, 2526-2532.
16 O. Syshchyk, V. A. Skryshevsky, O. O. Soldatkin and A. P. Soldatkin, *Biosens. Bioelectron.*, 2015, **66**, 89-94.
17 R. Nishiyabu, S. Ushikubo, Y. Kamiya and Y. Kubo, *J. Mater. Chem. A*, 2014, **2**, 15846-15852.
18 Y. Zhang, P. Zuo and B. C. Ye, *Biosens. Bioelectron.*, 2015, **68**, 14-19.
19 Z. Q. Tou, T. W. Koh and C. C. Chan, *Sens Actuators, B*, 2014, **202**, 185-193.
20 C. Díez-Gil, R. Martínez, I. Ratera, A. Tárraga, P. Molina and J. Veciana, *J. Mater. Chem.*, 2008, **18**, 1997-2002.
21 E. Coronado, J. R. Galán-Mascarós, C. Martí-Gastaldo, E. Palomares, J. R. Durrant, R. Villar, M. Gratzel and M. K. Nazeeruddin, *J. Am. Chem. Soc.*, 2005, **127**, 12351-12356.
22 P. Das, A. Ghosh, H. Bhatt and A. Das, *RSC Advances*, 2012, **2**, 3714-3721.
23 Z. Gu, M. Zhao, Y. Sheng, L. A. Bentolila and Y. Tang, *Anal. Chem.*, 2011, **83**, 2324-2329.
24 G. Aragay, H. Montón, J. Pons, M. Font-Bardía and A. Merkoi, *J. Mater. Chem.*, 2012, **22**, 5978-5983.
25 A. A. Shunkevich, Z. I. Akulich, G. V. Mediak and V. S. Soldatov, *React. Funct. Polym.*, 2005, **63**, 27-34.
26 L. Zhang, Z. Li, R. Chang, Y. Chen and W. Zhang, *React. Funct. Polym.*, 2009, **69**, 234-239.
27 M. A. A. Zaini, Y. Amano and M. Machida, *J. Hazard. Mater.*, 2010, **180**, 552-560.
28 G. Li, L. Zhang, Z. Li and W. Zhang, *J. Hazard. Mater.*, 2010, **177**, 983-989.

29 L. Zhang, X. Zhang, P. Li and W. Zhang, *React. Funct. Polym.*, 2009, **69**, 48-54.

30 O. P. Shvoeva, V. P. Dedkova and S. B. Savvin, *J. Anal. Chem.*, 2008, **63**, 1155-1157.

31 Y. Zhang, W. Xiang, R. Yang, F. Liu and K. Li, *J. Photochem. Photobiol., A*, 2005, **173**, 264-270.

32 H. Y. Luo, J. H. Jiang, X. B. Zhang, C. Y. Li, G. L. Shen and R. Q. Yu, *Talanta*, 2007, **72**, 575-581.

33 Y. Xu, L. Zhao, H. Bai, W. Hong, C. Li and G. Shi, *J. Am. Chem. Soc.*, 2009, **131**, 13490-13497.

34 C. Y. Li, X. B. Zhang, L. Qiao, Y. Zhao, C. M. He, S. Y. Huan, L. M. Lu, L. X. Jian, G. L. Shen and R. Q. Yu, *Anal. Chem.*, 2009, **81**, 9993-10001.

35 Z. X. Han, H. Y. Luo, X. B. Zhang, R. M. Kong, G. L. Shen and R. Q. Yu, *Spectrochim. Acta, Part A*, 2009, **72**, 1084-1088.

36 Y. Yang, J. Jiang, G. Shen and R. Yu, *Anal. Chim. Acta*, 2009, **636**, 83-88.

37 M. Shamsipur, M. Sadeghi, M. H. Beyzavi and H. Sharghi, *Mater. Sci. Eng. C*, 2015, **48**, 424-433.

38 R. Grigg and W. D. J. A. Norbert, *J. Chem. Soc.*, *Chem. Commun.*, 1992, 1298-1300.

39 S. Abad, M. Kluciar, M. A. Miranda and U. Pischel, *J. Org. Chem.*, 2005, **70**, 10565-10568.

40 Y. Q. Weng, F. Yue, Y. R. Zhong and B. H. Ye, *Inorg. Chem.*, 2007, **46**, 7749-7755.

41 Y. Cho, S. S. Lee and J. H. Jung, *Analyst*, 2010, **135**, 1551-1555.

42 L. Sun, Y. Li, M. Sun, H. Wang, S. Xu, C. Zhang and Q. Yang, *New J. Chem.*, 2011, **35**, 2697-2704.

43 G. Li, J. Xiao and W. Zhang, *Green Chem.*, 2011, **13**, 1828-1836.

44 H. Liu, N. Zang, F. Y. Zhao, K. Liu, Y. Li and W. J. Ruan, Wuli *Huaxue Xuebao/ Acta Phys-Chim Sin.*, 2014, **30**, 1801-1809.

45 W. J. Kruper Jr, T. A. Chamberlin and M. Kochanny, *J. Org. Chem.*, 1989, **54**, 2753-2756.

46 S. M. Badawy and A. M. Dessouki, *J. Phys. Chem. B*, 2003, **107**, 11273-11279.

47 R. X. Liu, B. W. Zhang and H. X. Tang, *React. Funct. Polym.*, 1999, **39**, 71-81.

48 A. Shirmardi-Dezaki, M. Shamsipur, M. Akhond and H. Sharghi, *J. Electroanal. Chem.*, 2013, **689**, 63-68.

49 C.-Y. Li, Y. Zhou, Y.-F. Li, X.-F. Kong, C.-X. Zou and C. Weng, *Anal. Chim. Acta*, 2013, **774**, 79-84.

50 S. Botasini, G. Heijo and E. Méndez, *Anal. Chim. Acta*, 2013, **800**, 1-11.

51. M. Biesaga, K. Pyrzyńska and M. Trojanowicz, *Talanta*, 2000, **51**, 209-224.

Table of Contents

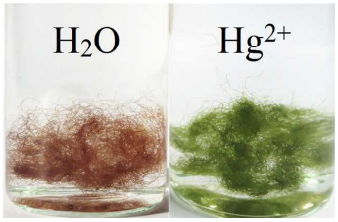

This colorimetric fiber sensor shows excellent selectivity and sensitivity towards Hg^{2+} over other common metal ions and can be repeatedly used for more than 50 times.